J Mol Model (2013) 19:1835–1851
DOI 10.1007/s00894-012-1742-3

ORIGINAL PAPER

Spectroscopic investigations and hydrogen bond interactions of 8-aza analogues of xanthine, theophylline and caffeine: a theoretical study

Mylsamy Karthika · Ramasamy Kanakaraju · Lakshmipathi Senthilkumar

Received: 10 October 2012 / Accepted: 17 December 2012 / Published online: 15 January 2013

Abstract The structure, spectral properties and the hydrogen bond interactions of 8-aza analogues of xanthine, theophylline and caffeine have been studied by using quantum chemical methods. The time-dependent density functional theory (TD-DFT) and the singly excited configuration interaction (CIS) methods are employed to optimize the excited state geometries of isolated 8-azaxanthine, 8-azatheophylline tautomers and 8-azacaffeine in both the gas and solvent phases. The solvent phase calculations are performed using the polarizable continuum model (PCM). The absorption and emission spectra are calculated using the time-dependent density functional theory (TD-DFT) method. The results from the TD-DFT calculations reveal that the excitation spectra are red shifted relative to absorption in aqueous medium. These changes in the transition energies are qualitatively comparable to the experimental data. The examination of molecular orbital reveals that the molecules with a small H→L energy gap possess maximum absorption and emission wavelength. The relative stability and hydrogen bonded interactions of mono and heptahydrated 8-azaxanthine, 8-azatheophylline tautomers and 8-azacaffeine have been studied using the density functional theory (DFT) and Møller Plesset perturbation theory (MP2) implementing the 6-311++G(d,p) basis set. The formation of strong N-H…O bond has resulted in the highest interaction energy among the monohydrates. Hydration does not show any significant impact on the stability of heptahydrated complexes. The atoms in molecule (AIM) and natural bonding orbital (NBO) analyses have been performed to elucidate the nature of the hydrogen bond interactions in these complexes.

Keywords AIM analysis · Excited state · Hydration · NBO analysis · TD-DFT

Introduction

Chemical modification of natural nucleobases opens a new field in the search for effective antiviral and antitumor therapy. One of these chemical changes in the modification of the imidazole ring of purines leads to 8-azapurine [1, 2], 8-azaguanine, 8-azaxanthines [3] and 8-azahypoxanthines [4–6]. Among the members of a series of carbocyclic purine nucleosides with antitumor activity, the corresponding 8-aza analogues are more active than the parent compounds [7]. The replacement of the C-H group in the imidazole ring of natural purines by a nitrogen atom produces a family of compounds named 8-azapurines [8]. 8-Azapurines have long been known to possess strong antipurine activity, i.e., antifungal, antiviral and anticancer properties [9, 10]. The presence of the nitrogen atom at position 8 provides an additional basic center which in turn affects the basicities of the other nitrogens of the ring, produces changes in the purine ring structure and induces glycosyl conformations of the corresponding nucleosides due to restricted rotation around this bond [11]. It seems quite clear that the replacement of a C-H group by a nitrogen atom produces a number of possibilities for both proton and metal coordination.

The chemical, physicochemical and biological properties of 8-azapurines have been comprehensively reviewed by Albert [8]. Both 8-azapurines and their nucleosides have

Electronic supplementary material The online version of this article (doi:10.1007/s00894-012-1742-3) contains supplementary material, which is available to authorized users.

M. Karthika · R. Kanakaraju (✉)
Department of Physics, NGM College, Pollachi 642 001, India
e-mail: rkanagu_1@rediffmail.com

L. Senthilkumar
Department of Physics, Bharathiar University,
Coimbatore 641 046, India

been widely studied as potential antimetabolites [12] and as model systems for elucidating the mechanisms of action of natural nucleosides and their analogues in various enzyme systems [13]. Considerable interest attaches to the finding that various analogues of 8-azaxanthine display interesting properties as antagonists of adenosine receptors [14]. Molecular orbital calculations have demonstrated that the substitution of C-H by N in position 8 of the purine ring causes a pronounced electron density withdrawal from this position, N8 bearing a rather small negative charge [15–18]. Furthermore, metal coordination to N3 has been observed in 8-azapurines [5] but it is not in purines.

Nubel and Pfleiderer [19] first reported the synthesis and properties of 8-azaxanthine and its various *N*-methyl derivatives. Prototropic tautomerism of 8-azatheophylline (1,3-dimethyl-8-azaxanthine) was subsequently investigated by Labbe et al. [20] by means of ^{13}C and ^{15}N NMR spectroscopy, with results pointing to predominance (80 %) of the N8-H form in dimethylsulfoxide (DMSO) solution, the sole form found for the parent neutral monohydrate of 8-azaxanthine, and other 8-azapurines, in the crystalline state [21]. Although the synthesis and physicochemical properties of 8-azapurines were long ago extensively reviewed by Albert [8], very little attention appears to have been directed to the fact that a number of these exhibit intrinsic fluorescence [22, 23]. 8-azaxanthine, the product of enzymatic deamination of the known cytotoxic agent 8-azaguanine [24] and an inhibitor of several key enzymes involved in purine metabolism [25–27] reveals strong intrinsic fluorescence in weakly acid medium, potentially useful in enzymological studies. The room-temperature fluorescence emission properties of 8-azatheophylline (1,3-dimethyl-8-azaxanthine) and 8-azacaffeine (1,3,7-trimethyl-8-azaxanthine) have been recently studied [28]. The spectral studies of macromolecular complexes with fluorescent ligands undergoing ground state tautomerism have been shown to provide information on hydrogen bonding patterns within the binding site [29, 30] and its possible changes.

The aim of the present work is to investigate the electronic structure, optical absorption, emission properties and the hydrogen bonded interactions of 8-azaxanthine, 8-azatheophylline (1,3-dimethyl-8-azaxanthine) tautomers and 8-azacaffeine (1,3,7-trimethyl-8-azaxanthine). The optical properties involve both occupied and unoccupied states. The time-dependent density functional theory (TD-DFT) [31, 32] and configuration interaction singles (CIS) [33] are the most popular quantum chemical methods used to calculate the excited state properties of medium-sized molecules. TD-DFT is a reliable method for the excited state computation [34] that provides accurate results. To the best of our knowledge there are no theoretical studies available on absorption, emission spectra and the hydrogen bonded interactions of 8-aza analogues of xanthine, theophylline tautomers and 8-azacaffeine. Hence, as a first part of the work, the absorption and emission properties have been studied by employing TD-DFT and CIS methods. As a second part of the work, the hydrogen bonded interactions have been analyzed for the ground state by interacting water molecule with all possible donor and acceptor sites of the molecules at MP2 and B3LYP level of theory using 6-311++G(d,p) basis set. In order to complete the first hydration shell, seven water molecules are placed at different hydrogen bond donor and acceptor sites of the molecule and hence two to six water molecules are not included in the present investigation.

A detailed molecular understanding of the energetic and geometric changes in the azacompounds would be a prerequisite in assessing their biological activity. The strong fluorescence should be useful for the studies of protein-ligand interactions. The interactions with water are particularly important because of water being universal solvent and its abundance in biological systems. The present theoretical study will also provide information about structural and other basic properties such as conformational stability, frontier molecular orbitals and dipole moment. The hydrogen bonding patterns of the complexes have been analyzed using the topological parameters calculated using AIM analysis based on Bader's atoms in molecules theory [35]. NBO analysis [36] has been performed to investigate the charge transfer interaction between the orbitals.

Computational details

The ground state geometries of isolated and hydrated complexes have been studied using the Becke's three parameter exact exchange functional (B3) [37] combined with gradient-corrected correlation functional of Lee-Yang-Parr (LYP) [38] of density functional theory, implementing 6-311++G(d,p) basis set. Harmonic vibrational frequencies are calculated at the same level of theory to characterize the stationary points. In order to achieve rigorous energy comparison, single point energy calculation has been performed at Møller-Plesset perturbation theory (MP2) [39] for the geometries optimized at B3LYP level of theory. The excited state geometry of isolated 8-azaxanthine, 8-azatheophylline tautomers and 8-azacaffeine are optimized at TD-B3LYP/6-311++G(d,p) [31, 32] and CIS/6-311++G(d,p) [33] level of theory. With the optimized ground and excited state geometries, the absorption and emission spectrum are calculated using TD-DFT method at B3LYP/6-311++G(d,p) level of theory. The ground, excited state optimization and spectral calculations are carried out in gas phase and in methanol, acetonitrile and water medium using Tomasi's [40] polarized continuum model (PCM) in self-consistent reaction field (SCRF) theory to compare with the available experimental results. In the PCM method, the

solute molecule is lying inside a cavity representing a solvent medium defined in terms of structureless material characterized by its dielectric constant, radius, density and molecular volume. Interaction energies have been corrected for the basis set superposition errors (BSSE), using the counterpoise method of Boys and Bernardi [41] for the hydrated complexes using B3LYP method with the 6-311++G(d,p) basis set. Topological analysis has been carried out using Morphy 98 software [42] for the optimized geometries. NBO analysis has been performed by using NBO 3.1 program at B3LYP level of theory. All the calculations have been carried out using the Gaussian 03W computational package [43].

Results and discussion

Structures and energies

The optimized molecular structures of 8-aza analogues of xanthine, theophylline and caffeine are depicted in Fig. 1. The two experimentally detectable protomeric forms of 8-azaxanthine and 8-azatheophylline are considered for the present study. For convenience, the optimized tautomers of 8-azaxanthine are labeled as AX1, AX2 and 8-azatheophylline as AT1 and AT2 and 8-azacaffeine as AC. The selected structural parameters of isolated 8-azaxanthine tautomers are summarized in Table 1. For 8-azatheophylline tautomers and 8-azacaffeine, the parameters are displayed as supplementary material in Tables S1 and S2. It has been observed that the structural parameters are significantly affected by the substitution of methyl group at 1, 3 and 7 position of 8-azaxanthine. Further, the calculated ground state geometrical parameters of AT1 tautomer are comparable with the available experimental data [21]. It can be observed that the N7 protonated optimized geometry of 8-azatheophylline (AT2) is in good agreement with the available X-ray diffraction data obtained for 1,3-dimethyl-8-azaxanthine monohydrate. As there is no experimental data available for AC, a comparison of bond angles in the triazole ring of AC with the available experimental data of different azapurines have been made [21] and the deviations is trivial ranging from 0.1-0.4°.

The total energies calculated using MP2/6-311++G(d,p) and B3LYP/6-311++G(d,p) level of theory summarized in Table 2 shows that at all applied levels, the N8 protonated tautomer of 8-azaxanthine (AX1) and 8-azatheophylline (AT1) are the global minimum on the potential energy surface, which are in agreement with the earlier studies on the solid state [20, 21]. The order of stability of two protomeric forms of 8-azaxanthine is AX1 >AX2 and that of 8-azatheophylline is AT1>AT2 calculated at MP2/6-311++G(d,p) and B3LYP/6-311++G(d,p) level of theory. The solute-solvent interactions are taken into account by applying SCRF theory. The results indicate that the solvent does not alter the stability of the tautomers however, a significant change in energy could be predicted in the solvent phase. It is important to understand the energetic changes caused by the substitution of nitrogen in the place of imidazole C-H of xanthine and theophylline. Previous studies on xanthine [44] at MP2/6-31G** level of theory suggested that N7-H prototropic tautomer to be more stable than N9-H by 8.35 kcal mol^{-1}. Further, among theophylline tautomers studied by Smith et al. [45] the lowest energy tautomer is the N7-H form, while the N9-H tautomer is 9 kcal mol^{-1} higher in energy. Thus the substitution of nitrogen for C-H of xanthine and theophylline decreases the energy difference between the most stable tautomers.

Absorption properties

The spectral studies of isolated 8-azaxanthine, 8-azatheophylline tautomers and 8-azacaffeine have been performed using TD-DFT at B3LYP/6-311++G(d,p) level of theory in gas and solvent phases. The calculated absorption energy, corresponding oscillator strength and orbital coefficients together with the experimental values of Medza et al. [28] are summarized in Table 3 for gas phase (ε=1) and in methanol (ε=32.63) medium. To obtain the nature and energy of the singlet-singlet electronic transition, the predictions of the first 10 excited states are performed within the TD-DFT formalism. The absorption energies with oscillator strength greater than 0.01 are considered throughout the discussion. It has been observed that for all the studied molecules, the absorption wavelength calculated in gas phase and in solvent phases (methanol, acetonitrile and water) is nearly similar and the maximum variation is only around 0.16 eV. As the polar environment does not influence the absorption spectrum and oscillator strength of 8-aza compounds, the absorption spectrum calculated in methanol medium has been discussed in detail.

The TD-DFT results show that for all the isolated complexes, the lowest energy transition is due to the excitation of electron from highest occupied molecular orbital (HOMO) to the lowest unoccupied molecular orbital (LUMO). The absorption intensity is directly related with the dimensionless oscillator strength and the dominant absorption bands are the transitions with higher oscillator strength value. The absorption energies calculated at TD-B3LYP/6-311++G(d,p) level of theory in gas phase and methanol medium are plotted with respect to oscillator strength and shown in Fig. 2. The curves corresponding to acetonitrile and water are given as supplementary information in Fig. S1. The absorption spectra agree well with the previous experimental values [28].

In methanol, the absorption spectrum of AX1 and AX2 has two peaks with the dominant absorption band of AX1 observed at 4.86 eV (255 nm), which is associated with the

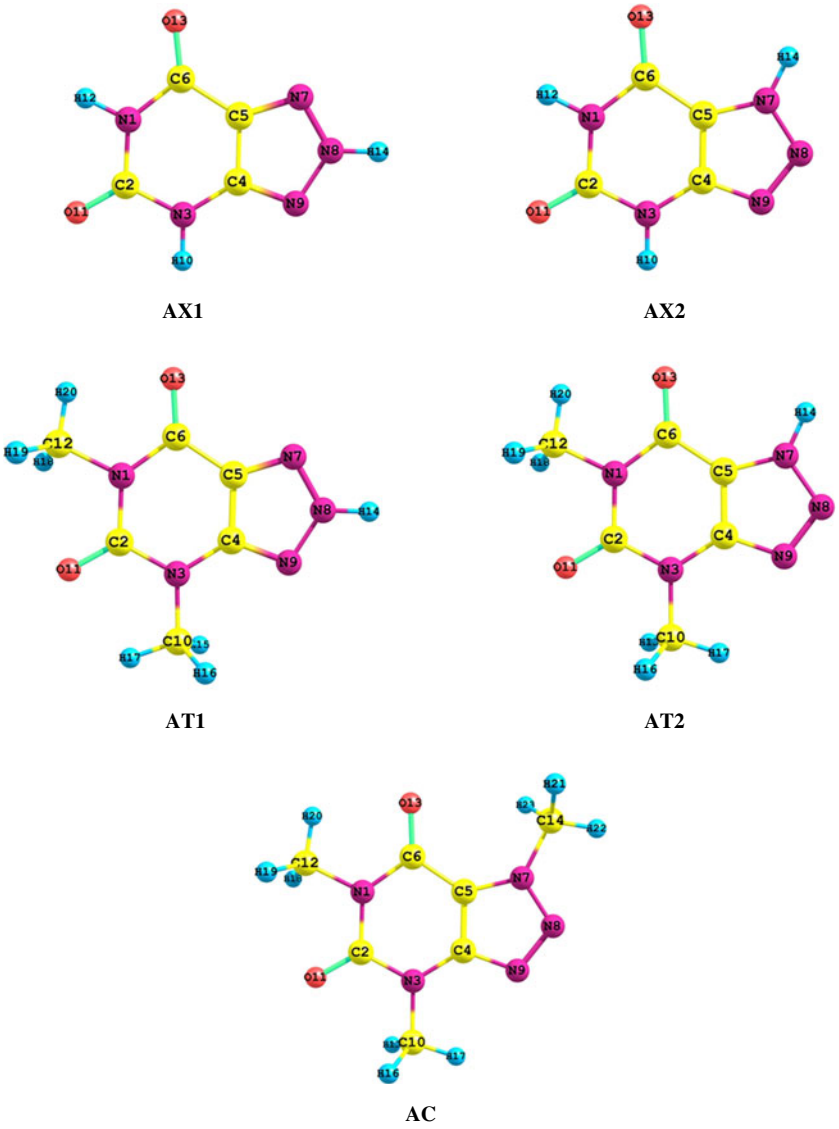

Fig. 1 The optimized structures of isolated 8-azaxanthine tautomers (AX1, AX2), 8-azatheophylline tautomers (AT1, AT2) and 8-azacaffeine (AC)

H(HOMO)→L (LUMO) transition. The second intense band is observed around 5.68 eV (218 nm) which corresponds to H-2→L transition. The absorption spectrum of AX2 possesses one intense peak at 4.67 eV (267 nm), associated with H→L transition and one less intense peak around 5.81 eV (216 nm) related with H-3→L transition. The absorption maxima (λ_{max}) of AT1 and AT2 exhibit a red shift of about 10 nm compared with the λ_{max} of AX1 and AX2. Thus the substitution at 1st and 3rd position of 8-azaxanthine with an electron - donating group increases the absorption energy. It is also interesting to note that the N7 protonated tautomers in 8-azaxanthine and 8-azatheophylline exhibit a red shift compared to N8 protonated tautomers. The absorption maxima (λ_{max}) of AC are also found to exhibit a red shift of about 9 nm compared with the λ_{max} of AX2. Further, AC has the same spectral features as those of the N7 protonated AT2 tautomer. Replacement of the hydrogen atom at position 7 by a methyl group does not influence the spectrum appreciably.

Emission properties

The excited state geometry of AX1, AX2, AT1, AT2 and AC have been optimized by using the TD-B3LYP and singly excited configuration interaction (CIS) methods with the 6-311++G(d,p) basis set in gas and solvent phases. Along with the available experimental results, the calculated emission wavelength and the corresponding oscillator strength calculated at TD-B3LYP/6-311++G(d,p) level of theory are summarized in Table 4 for gas phase and methanol. 8-azaxanthine is virtually non-fluorescent in neutral aqueous medium, but below pH 6 it begins to emit, with strong fluorescence, centered at about 420 nm. By contrast when 8-azaxanthine is dissolved in anhydrous methanol, acidified with 1mM acetic acid, the fluorescence maximum was shifted to 335 nm [46]. 8-azatheophylline is a highly fluorescent compound, with λ_{max}~353 nm and 8-azacaffeine is only weakly fluorescent in aqueous medium with λ_{max}~350 nm. Its fluorescence

Table 1 Selected geometrical parameters (bond length in Å, angle in degrees) of AX1 and AX2 calculated at B3LYP/6-311++G(d,p) and TD-B3LYP/6-311++G(d,p) level of theory in gas phase[a]

Parameters	AX1		AX2	
	Ground state	Excited state	Ground state	Excited state
N3-C2	1.389	1.378	1.388	1.402
N3-C4	1.372	1.382	1.372	1.368
N3-H10	1.010	1.010	1.010	1.014
N1-C2	1.401	1.403	1.406	1.357
N1-C6	1.412	1.391	1.406	1.463
N1-H12	1.013	1.011	1.013	1.012
C2-O11	1.210	1.212	1.210	1.228
C4-C5	1.407	1.424	1.376	1.420
C4-N9	1.326	1.305	1.353	1.335
C5-C6	1.462	1.381	1.448	1.425
C5-N7	1.336	1.367	1.359	1.346
C6-O13	1.208	1.315	1.214	1.228
N7-N8	1.314	1.352	1.336	1.460
N7-H14	–	–	1.011	1.009
N9-N8	1.010	1.363	–	–
N8-H14	1.345	1.005	1.313	1.309
C2-N3-C4	121.0	122.1	121.0	121.7
C2-N3-H10	117.0	116.7	117.4	116.3
N3-C2-N1	114.6	114.7	114.4	116.7
N3-C2-O11	122.9	124.2	123.4	118.3
C4-N3-H10	122.0	121.2	121.6	122.0
N3-C4-C5	122.4	121.4	121.8	119.5
N3-C4-N9	127.8	127.8	128.2	128.3
C2-N1-C6	130.6	126.1	130.0	127.9
C2-N1-H12	113.9	114.6	114.0	116.2
N1-C2-O11	122.5	121.1	122.2	125.0
C6-N1-H12	115.5	119.4	115.9	115.9
N1-C6-C5	110.0	117.5	109.7	110.3
N1-C6-O13	121.7	114.5	122.8	120.0
C5-C4-N9	109.8	110.8	110.0	112.2
C4-C5-C6	121.4	118.3	123.0	123.9
C4-C5-N7	108.2	108.4	103.1	101.9
C4-N9-N8	101.6	102.3	107.5	109.5
C6-C5-N7	130.4	133.3	133.8	134.1
C5-C6-O13	128.3	128.1	127.5	129.7
C5-N7-N8	102.9	101.2	110.9	110.8
N7-N8-N9	117.5	117.3	108.4	105.5
N7-N8-H14	121.6	121.7	–	–
N9-N8-H14	120.9	121.0	–	–
C5-N7-H14	–	–	128.9	128.9
N8-N7-H14	–	–	120.2	120.0

[a] For labeling of atoms see Fig. 1

Table 2 Total energy E_{tot} (Hartree) and ground state dipole moment μ_m (Debye) of isolated 8-azaxanthine, 8-azatheophylline and 8-azacaffeine calculated at MP2/6-311++G(d, p) and B3LYP/6-311++G (d, p) level of theory in gas and solvent phases

Medium	System	MP2/6-311 ++G(d,p)		B3LYP/6-311 ++G(d,p)	
		E_{tot}	μ_m	E_{tot}	μ_m
Gas (ε=1)	AX1	−577.1281	4.24	−578.6099	3.98
	AX2	−577.1248	1.68	−578.6064	1.26
	AT1	−655.5095	3.75	−657.2464	3.59
	AT2	−655.5076	0.71	−657.2438	0.29
	AC	−694.7050	1.66	−696.5685	1.29
Methanol (ε=32.63)	AX1	−577.1664	5.95	−578.6494	5.77
	AX2	−577.1635	2.24	−578.6461	1.73
	AT1	−655.5330	5.47	−657.2707	5.37
	AT2	−655.5307	1.52	−657.2677	1.04
	AC	−694.7192	2.07	−696.5837	1.65
Acetonitrile (ε=36.64)	AX1	−577.1665	5.97	−578.6496	5.79
	AX2	−577.1636	2.25	−578.6462	1.74
	AT1	−655.5330	5.47	−657.2708	5.37
	AT2	−655.5307	1.52	−657.2678	1.04
	AC	−694.7191	2.08	−696.5837	1.65
Water (ε=78.39)	AX1	−577.1678	6.03	−578.6509	5.85
	AX2	−577.1650	2.25	−578.6476	1.74
	AT1	−655.5341	5.54	−657.2718	5.44
	AT2	−655.5317	1.56	−657.2688	1.09
	AC	−694.7198	2.09	−696.5845	1.67

excitation spectrum is slightly red shifted relative to its UV absorption spectrum possibly due to cage effect [47].

For 8-azaxanthine, 8-azatheophylline tautomers and 8-azacaffeine, the emission energies calculated at TD-B3LYP/6-311++G(d,p) level of theory in gas phase and in methanol medium are plotted with respect to oscillator strength and is shown in Fig. 3. The curves corresponding to acetonitrile and water are given as supplementary information in Fig. S2. It has been observed that the emission spectra calculated for AX1, AX2, AT1, AT2 and AC in solvent phase are nearly identical and are found to be different from the gas phase. Significant deviations have been observed for AT2 in water and AC in acetonitrile compared to methanol. Further, it has been observed that the emission wavelength calculated through TD-B3LYP method in solvent phase are in agreement with the experimental values [28, 46] where, excitation spectra are red-shifted relative to absorption in methanol and acetonitrile medium. The emission energies calculated at gas phase for AX1 exhibit two peaks, the maximum peak is observed at 4.60 eV (279 nm) associated with H→L transition and second peak at 5.56 eV (255 nm) corresponding to H-1→L transition. For AX2, the emission spectrum is

Table 3 Available experimental values and computed absorption energy λ (in nm and in eV) and oscillator strengths f (in a.u.) of isolated 8-azaxanthine, 8-azatheophylline and 8-azacaffeine calculated at TD-B3LYP/6-311++G(d,p)//B3LYP/6-311++G(d,p) level of theory in gas and methanol medium

System	Gas(ε=1)				Methanol(ε=32.63)				
	Orbital transitions	Absorption energy(λ)		Oscillator strength f(a.u.)	Orbital transitions	Expt[a]	Absorption energy(λ)		Oscillator strength f(a.u.)
		nm	eV				nm	eV	
AX1	H->L(0.654)	255	4.71	0.11	H->L(0.654)	263	255	4.86	0.11
	H-2->L(0.611)	217	5.50	0.04	H-2->L(0.615)		218	5.68	0.05
	H->L+1(0.471)	200	5.93	0.05					
AX2	H->L(0.643)	268	4.52	0.10	H->L(0.644)	263	267	4.67	0.10
	H-3->L(0.603)	214	5.58	0.05	H-3->L(0.608)		216	5.81	0.06
	H->L+2(0.424)	202	5.89	0.04					
AT1	H->L(0.657)	266	4.68	0.11	H->L(0.657)	271	265	4.79	0.11
	H-2->L(0.644)	233	5.35	0.04	H-2->L(0.644)		233	5.48	0.04
	H->L+2(0.531)	205	6.11	0.10					
AT2	H->L(0.646)	278	4.46	0.11	H->L(0.646)	271	277	4.56	0.11
	H-2->L(0.645)	230	5.40	0.05	H-2->L(0.646)		230	5.54	0.05
	H->L+2(0.497)	207	6.00	0.06					
AC	H->L(0.647)	277	4.54	0.11	H->L(0.647)	280	276	4.59	0.10
	H-2->L(0.631)	228	5.56	0.06	H-2->L(0.630)		227	5.64	0.06
	H-4->L(0.427)	208	6.09	0.03					

[a]Taken from ref [28]

observed at 4.88 eV (320 nm) and 7.41 eV (238 nm) associated with H→L and H-2→L transition. The N8 protonated 8-azaxanthine tautomer AX1 exhibits sharp intense peak than N7 protonated AX2 tautomer. For AT1, two emission peaks are observed similar to AX1 and AX2, with maximum emission observed around 6.12 eV (291 nm) and 6.92 eV (266 nm) associated with H→L and H-1→L transitions, respectively. In AT2, the maximum peak is observed at 4.74 eV (334 nm) corresponding to H→L transition and second peak at 6.92 eV (256 nm) associated with H-2→L transition. The substitution of methyl group for hydrogen at 1st and 3rd position of 8-azaxanthine has resulted in the shift of intense spectra to higher wavelengths indicating the influence of methyl group over the substitution. Further, as noted for 8-azaxanthine tautomers, N8 protonated AT1 tautomer exhibits sharp intense peak than N7 protonated AT2 tautomer. The substitution of methyl group at triazole nitrogen N7 in AC does not influence the emission spectra significantly.

As shown in Fig. 3, the emission spectrum calculated in methanol medium for 8-azaxanthine exhibits three peaks, with the emission maximum (λ_{max}) of AX1 and AX2 at 4.00 eV (307 nm) and 3.85 eV (317 nm), respectively which is associated with H→L transition. In comparison with 8-azaxanthine, the λ_{max} of 8-azatheophylline is red shifted by about 20 nm (AT1) and 11 nm (AT2). This is in accordance with the previously postulated phototautomeric behavior of 8-azaxanthine [46]. The substitution of methyl group at 1st and 3rd positions of 8-azaxanthine influences the spectral properties however, no significant change has been noted due to protomerization. The observed emission spectra results in highly intense peak in solvent medium than gas phase indicating the solvent dependency of the observed spectra. As observed for AT1 and AT2,

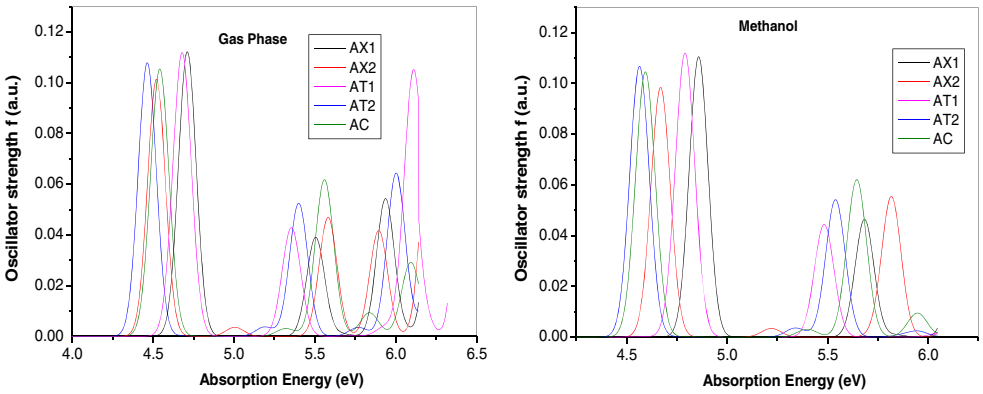

Fig. 2 The absorption spectra of AX1, AX2, AT1, AT2 and AC in gas and methanol medium computed at TD-B3LYP/6-311++G(d,p)//B3LYP/6-311++G(d,p) level of theory

Table 4 Available experimental values and computed emission energy λ (in eV and in nm) and oscillator strengths f (in a.u.) of isolated 8-azaxanthine, 8-azatheophylline and 8-azacaffeine calculated at TD-B3LYP/6-311++G(d,p) level of theory in gas and methanol medium

System	Gas(ε=1)				Methanol(ε=32.63)				
	Orbital transitions	Emission energy(λ)		Oscillator strength f(a.u.)	Orbital transitions	Expt	Emission energy(λ)		Oscillator strength f(a.u.)
		nm	eV				nm	eV	
AX1	H->L(0.668)	279	4.60	0.12	H->L(0.680)	335[a]	307	4.00	0.09
	H-1->L(0.665)	255	5.56	0.04	H-2->L(0.607)		234	5.21	0.05
					H->L+1(0.523)		212	5.76	0.05
AX2	H->L(0.693)	320	4.88	0.09	H->L(0.693)	335[a]	317	3.85	0.10
	H-2->L(0.672)	238	7.41	0.06	H-2->L(0.666)		234	5.18	0.05
					H->L+1(0.522)		213	5.66	0.05
AT1	H->L(0.686)	291	6.12	0.11	H->L(0.697)	353[b]	327	3.78	0.09
	H-1->L(0.683)	266	6.92	0.05	H-2->L(0.679)		256	4.82	0.05
					H->L+1(0.457)		218	5.69	0.04
AT2	H->L(0.695)	334	4.74	0.10	H->L(0.695)	353[b]	328	3.75	0.11
	H-2->L(0.686)	256	6.92	0.06	H-2->L(0.679)		249	4.88	0.05
					H->L+2(0.563)		217	5.61	0.04
AC	H->L(0.676)	339	4.73	0.10	H->L(0.632)	350[b]	336	3.69	0.11
	H-2->L(0.690)	250	7.36	0.06	H-1->L(0.645)		247	5.03	0.06
					H->L+3(0.450)		219	5.65	0.04

[a] Taken from ref [46]

[b] Taken from ref [28]

the emission spectrum of AC is also red shifted by about 19 nm relative to 8-azaxanthine AX2 and 10 nm relative to AT2 as a result of the methyl substitution. The observed emission in AC is also observed to be solvent dependent. The emission energies calculated for acetonitrile does not show a larger variation compared to methanol however, the observed spectrum is found to be close to the experimental observations [28]. Further, the neutral aqueous medium influences the spectrum appreciably resulting in additional transitions that could be observed for AX1, AT1, AT2 and AC.

The emission energies calculated at TD-B3LYP//6-311++G(d,p)//CIS/6-311++G(d,p) level of theory for gas and solvent phases show a larger variation compared to TD-DFT level of theory (see Table S3 and Fig. S3). A number of orbital transitions could be observed in acetonitrile and water medium compared to methanol. It is to be noted that the emission energy calculated at TD-B3LYP/6-311++G(d,p) level of theory closely agrees with the experimental values [28, 46] compared to CIS/6-311++G(d,p) level of theory.

Frontier molecular orbitals

The density plot of the HOMO and LUMO of 8-azaxanthine, 8-azatheophylline tautomers and 8-azacaffeine for the ground and excited states in the gas phase calculated at B3LYP/6-311++G(d,p) level of theory are shown in Fig. S4. The orbital diagrams

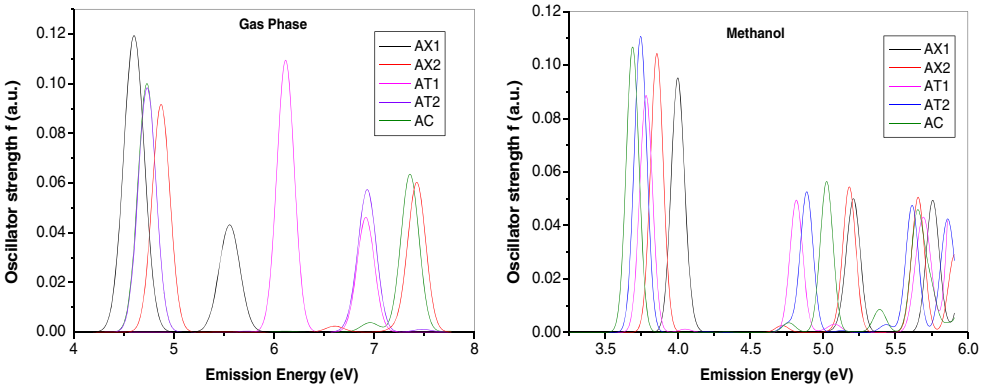

Fig. 3 The emission spectra of AX1, AX2, AT1, AT2 and AC in gas and methanol medium computed at TD-B3LYP /6-311 ++G(d,p) level of theory

are plotted with the contour value of 0.05 a.u. The plots of the HOMO and LUMO of the studied molecules have the typical π-molecular orbital characteristics and are slightly altered by the substitution. From the molecular orbital analysis, it is inferred that the lowest lying singlet-singlet absorption as well as emission corresponds to the electronic transition of $\pi \rightarrow \pi^*$ type. The ground and excited state molecular orbital energies have been calculated at the TD- B3LYP/ 6-311++G(d,p) level of theory in the gas phase and are summarized in Table 5. The calculated H-L energy gap for the ground state of isolated AX1 and AX2 in gas phase is found to be 5.37 and 5.10 eV, respectively. It has been observed that the H-L energy gap slightly decreases upon the substitution of methyl group in the 8-azaxanthine molecule. The H→L energy gap of AT1 and AT2 is lesser than AX1 and AX2 by 17-20 eV. As expected, the molecules with a small H→L energy gap possess maximum absorption and emission wavelengths. Similar observations could also be noted in the solvent phase. Among 8-azaxanthine tautomers AX1 and AX2, AX2 has a minimum H-L energy gap of 5.10 eV and hence a maximum absorption and emission wavelength of 268 nm (4.52 eV) and 320 nm (4.88 eV) in the gas phase. Similarly among 8-azatheophylline tautomers, AT2 has a minimum energy gap (4.93 eV) with a maximum absorption of 278 nm (4.46 eV) and emission of 334 nm (4.74 eV). Similar observations could be noted in methanol where, AX2 has a minimum H→L energy gap of 5.11 eV and hence a maximum absorption of 267 nm (4.67 eV) and emission of 317 nm (3.85 eV). Further, as noted in gas phase AT2 is said to have a minimum band gap of 4.93 eV among 8-azatheophylline tautomers and hence a maximum absorption and emission wavelength of 277 nm (4.56 eV) and 328 nm (3.75 eV), respectively. Further, it is interesting to note that the absorption and emission energy calculated at the TD-B3LYP/6-311++G(d,p) level of theory corresponding to the HOMO→-LUMO transition is comparable with the energy gap value. The same trend could be observed in acetonitrile and water medium. The above results show that the substitutions alter the spatial charge distribution of the frontier molecular orbitals, and hence the spectral properties depend on the substitution.

Table 5 Ground state molecular orbital energies (E_{HOMO}, E_{LUMO}) and energy gap (ΔE in eV) of isolated 8-azaxanthine, 8-azatheophylline and 8-azacaffeine molecules calculated at the B3LYP/6-311++G(d,p) level of theory in gas and methanol medium

Molecule	Gas(ε=1)			Methanol(ε=32.63)		
	E_{HOMO}	E_{LUMO}	ΔE	E_{HOMO}	E_{LUMO}	ΔE
AX1	−7.58	−2.21	5.37	−7.59	−2.22	5.37
AX2	−7.51	−2.41	5.10	−7.52	−2.41	5.11
AT1	−7.15	−1.98	5.17	−7.18	−1.98	5.20
AT2	−7.07	−2.14	4.93	−7.09	−2.14	4.95
AC	−6.89	−1.95	4.95	−6.91	−1.95	4.96

Structures and energies of mono and heptahydrated complexes

The two protomeric forms of 8-azaxanthine, 8-azatheophylline and 8-azacaffeine molecules offer several possible donor and acceptor sites to form hydrogen bonds. Therefore, to identify the actual site for hydrogen bond formation, monomers of 8-aza analogues have been allowed to interact with water molecules. The hydrogen bonding capability of 8-azaxanthine includes four hydrogen bond acceptors, two carbonyl oxygens of pyrimidine ring and two basic nitrogen of triazole group and in addition, it possesses three donors, two N-H groups of pyrimidine ring and a good N-H hydrogen bond donor of triazole group. 8-azatheophylline possesses a total of four sites that can act as hydrogen bond acceptors. Two groups are the triazole nitrogens and the remaining two groups are the carbonyl oxygen atoms of urea and amide moiety. Also it possesses a good N-H hydrogen bond donor of triazole group and two weak donors of methyl hydrogens. 8-azacaffeine comprises four sites that can act as hydrogen bond acceptors and three weak proton donors of methyl group.

After optimization of monomers, initial configurations of 8-azaxanthine, 8-azatheophylline and 8-azacaffeine monohydrates and heptahydrates are constructed with the water molecule positioned in the vicinity of the most reactive sites of their polar groups and are shown in Figs. S5–S9. Strong hydrogen bonds are formed between azacomplexes and water molecules. The optimized structures of monohydrated AX1 tautomer are labeled AX1…H_2O(a), AX1…H_2O(b), AX1…H_2O(c), AX1…H_2O(d), AX1…H_2O(e) and AX1…H_2O (f). The stable monohydrates of other tautomers are named in a similar manner. To complete the first hydration shell, seven water molecules are placed on all possible sites and the optimized complexes are named AX1…$(H_2O)_7$ and AX2…$(H_2O)_7$ for 8-azaxanthine , AT1…$(H_2O)_7$ and AT2…$(H_2O)_7$ for 8-azatheophylline and AC…$(H_2O)_7$ for 8-azacaffeine. Studying all these complexes together at the same level of theory allows us to analyze their relative stability in terms of the properties of the binding sites.

The systems analyzed here are coupled through N-H…O, O-H…N, O-H…O and C-H…O type hydrogen bonds. In a large number of complexes, the C8-H site is involved in a comparatively weak interaction with the water molecule. It is to be noted that N-H…O, O-H…N and C-H…O bonds in the majority of the heptahydrated complexes are found to be stronger than monohydrated complexes. It is to be observed that the X-H (X=N, O, C) bond length has been elongated from its corresponding monomer in all the complexes upon hydration. This elongation has resulted in a positive change in bond length (ΔR_{X-H}). The analysis reveals that the proton donor N-H involved in the interaction is elongated between values ranging from 0.0092-0.0172 Å for monohydration, the corresponding N-H…O bond in heptahydrated complexes

vary between 0.0129-0.0560 Å (Tables 7 and S4). This largest elongation corresponds to the smallest N-H… O intermolecular distance of 1.840 to 2.031 Å (monohydration) and 1.581 to 1.929 Å (heptahydration). Notably, the hydration at triazole nitrogen N8 of AX1…H_2O (d) results in a shorter bond length upon monohydration and at triazole nitrogen N7 of AX2…$(H_2O)_7$ upon heptahydration. Calculated bond angle shows that the hydrogen bonds are almost linear. In general, hydrogen bond angle for strong hydrogen bond ranges from 170-180° [48]. The shorter the distance and closer the angle to 180°, stronger is the hydrogen bond interaction. In the present study, the intermolecular angle for N-H…O is found to be much linear than other hydrogen bonds.

Interaction energy and relative stability

The interaction energy has been calculated after correcting the basis set superposition error (BSSE) by the full counterpoise procedure (CP) of Boys and Bernardi [41] using the equation:

$$E_{int}(corr) = E_{AB}(AB) - [E_A(AB) + E_B(AB)],$$

where E_{AB}(AB) is the energy of the complex, E_A(AB) and E_B(AB) are the energies of monomers A and B with the full complex basis set by setting the appropriate nuclear charge to zero, which is located at the same intermolecular configuration as in the complex.

Among AX1 monohydrates, the highest interaction energy (Table 6) has been predicted for AX1…H_2O(b) which is 8.85 kcal mol^{-1} at MP2/6-311++G(d,p) and 9.60 kcal mol^{-1} at B3LYP/6-311++G(d,p) level of theory. The most effective interaction of N8 protonated tautomer AX1 with the water molecule takes place on the pyrimidine nitrogen N3-H side of the molecule (Fig. S5) resulting in the strengthening of N-H…O bonds (1.925 Å) and hence a higher interaction energy value. The order of stability among monohydrated AX1 tautomer is AX1…H_2O(b) > AX1…H_2O(d) > AX1…H_2O(a) > AX1…H_2O(f) > AX1…H_2O(c) > AX1…H_2O(e) at MP2 and AX1…H_2O(b) > AX1…H_2O(a) ≈ AX1…H_2O(f) > AX1…H_2O(d) > AX1…H_2O(c) > AX1…H_2O(e) at B3LYP level of theory. However, the most and the least stable complexes agree at both levels of theory.

Among the monohydrated AX2 tautomer, the search of stable complexes also includes seven initial geometries that reproduce all possible hydrogen bonds and the optimizations converged to five stable monohydrates as presented in Fig. S6. Five closed complexes, which act as a proton donor and acceptor simultaneously, are formed. The location of water is the as same as that of the AX1 tautomer except AX2…H_2O(e) which differ in the character of the hydrogen bonds because of the different location of the hydrogen atom relative to the nitrogen in the triazole ring. An analysis of hydrogen bonds in N7 protonated AX2 monohydrates indicates the strengthening of the interaction energy compared to monohydrates of other complexes. This assumption agrees well with the values of the interaction energy (Table 6). The complex AX2…H_2O(e) is associated with maximum interaction energy of 11.61 and 12.41 kcal mol^{-1} at MP2/6-311++G(d,p) and B3LYP/6-311++G(d,p) level of theory, respectively. It is the largest interaction energy revealed in the present study. The formation of strong N7-H14…O15 bond (1.865 Å) is responsible for the stability of the complex. The order of stability among monohydrated AX2 tautomer is AX2…H_2O(e) > AX2…H_2O(c) > AX2…H_2O(b) > AX2…H_2O(a) > AX2…H_2O(f) at MP2 and AX2…H_2O(e) > AX2…H_2O(b) > AX2…H_2O(c) > AX2…H_2O(a) > AX2…H_2O(f) at B3LYP level of theory. The strength of the hydrogen bond observed in AX2 tautomer is found to be stronger than AX1 and hence a higher interaction energy.

The optimization of monohydrated AT1 tautomer has converged to five stable monohydrates as presented in Fig. S7. Significant changes are found in the geometry of the hydrogen bonds and interaction energy of 8-azatheophylline-water complex. The water molecule forms an open complex except AT1…H_2O(e) and AT1…H_2O(f). The highest interaction energy has been predicted for AT1…H_2O(d) of 7.66 and 7.53 kcal mol^{-1} at MP2 and B3LYP level of theory, respectively (Table 6). The highest interaction energy is due to the formation of strong N8-H14…O21 bond. Furthermore, the complex AT1…H_2O(c) is said to possess the minimum interaction energy among the monohydrates. Hence, the order of interaction energy is AT1…H_2O(d) > AT1…H_2O(b) > AT1…H_2O(e) > AT1…H_2O(f) > AT1…H_2O(c) at both levels of theory.

In N7 protonated AT2 tautomer, all the 6 stable monohydrates (Figure S8) form a closed complex and it is prominent that the location of the water molecule in these hydrates is almost identical with the respective complexes of the AT1 tautomer. However, the monohydrates AT2…H_2O(b) and AT2…H_2O(c) are stabilized by the secondary C–H…O bond formed with the participation of the methyl group. The maximum interaction energy has been observed for AT2…H_2O(e) (11.48 kcal mol^{-1}) at MP2/6-311++G(d,p) and 12.36 kcal mol^{-1} at B3LYP/6-311++G(d,p) level of theory (Table 6). The formation of two strong intermolecular hydrogen bonds between the triazole nitrogen N7-H and water (N-H…O) and carbonyl oxygen of amide moiety with water (O-H…O) results in the stabilization of the above complex. Notice that this complex is characterized by the shortest bond length equal to 1.859 and 1.888 Å. The order of interaction energy is AT2…H_2O(e) > AT2…H_2O(d) > AT2…H_2O(c) > AT2…H_2O(b) > AT2…H_2O(a) > AT2…H_2O(f) at both levels of theory. Hence, it is to be noted that the N7 protonated tautomers of 8-azaxanthine and 8-azatheophylline result in the highest interaction energy than N8 protonated tautomers. Further, it is interesting to note that the N7 protonated forms result only in closed complexes in 8-azaxanthine and 8-azatheophylline tautomers. On comparison with available monohydrated N7-H tautomer of theophylline studied by Balbuena et al. [49], the

Table 6 Total energy E_{tot} (Hartree), BSSE corrected interaction energy E_{int} (kcal mol^{-1}) and ground state dipole moment μ_m (Debye) of hydrated 8-azaxanthine, 8-azatheophylline and 8-azacaffeine complexes calculated at MP2/6-311++G(d,p) and B3LYP/6-311++G(d,p) level of theory

Complex	E_{tot}		E_{int}		μ_m	
	MP2	B3LYP	MP2	B3LYP	MP2	B3LYP
AX1…(H_2O)a	−653.4178	−655.0821	−7.59	−8.22	4.30	4.10
AX1…(H_2O)b	−653.4201	−655.0843	−8.85	−9.60	3.57	3.47
AX1…(H_2O)c	−653.4177	−655.0811	−7.40	−7.47	6.28	5.93
AX1…(H_2O)d	−653.4189	−655.0824	−8.03	−7.84	7.06	6.73
AX1…(H_2O)e	−653.4133	−655.0769	−4.83	−4.77	5.66	5.62
AX1…(H_2O)f	−653.4177	−655.0808	−7.53	−8.22	3.93	5.36
AX1…(H_2O)$_7$	−1111.1763	−1113.9333	−64.32	−68.65	6.36	5.98
AX2…(H_2O)a	−653.4153	−655.0792	−8.03	−8.53	1.13	1.10
AX2…(H_2O)b	−653.4164	−655.0805	−8.66	−9.41	1.04	1.15
AX2…(H_2O)c	−653.4172	−655.0801	−9.16	−9.10	3.49	2.87
AX2…(H_2O)e	−653.4211	−655.0852	−11.61	−12.41	2.49	2.40
AX2…(H_2O)f	−653.4144	−655.0786	−7.47	−8.16	3.08	2.78
AX2…(H_2O)$_7$	−1111.1761	−1113.9319	−67.90	−71.66	2.35	2.13
AT1…(H_2O)b	−731.7957	−733.7143	−5.65	−5.71	1.99	1.82
AT1…(H_2O)c	−731.7931	−733.7119	−4.02	−3.97	3.50	3.07
AT1…(H_2O)d	−731.7999	−733.7182	−7.66	−7.53	6.07	5.78
AT1…(H_2O)e	−731.7955	−733.7142	−5.52	−5.27	5.83	5.89
AT1…(H_2O)f	−731.7942	−733.7134	−4.89	−5.08	5.61	5.37
AT1…(H_2O)$_7$	−1189.5465	−1192.5514	−54.63	−55.03	2.97	3.03
AT2…(H_2O)a	−731.7931	−733.7113	−5.27	−5.27	2.39	1.99
AT2…(H_2O)b	−731.7936	−733.7117	−5.40	−5.52	1.86	1.98
AT2…(H_2O)c	−731.7946	−733.7125	−6.02	−5.84	2.74	2.36
AT2…(H_2O)d	−731.7975	−733.7146	−7.91	−7.22	2.93	2.36
AT2…(H_2O)e	−731.8038	−733.7225	−11.48	−12.36	1.99	2.09
AT2…(H_2O)f	−731.7917	−733.7105	−4.52	−4.77	2.68	2.12
AT2…(H_2O)$_7$	−1189.5382	−1192.5493	−53.53	−56.66	5.60	5.83
AC…(H_2O)a	−770.9908	−773.0362	−5.40	−5.40	2.68	2.24
AC…(H_2O)b	−770.9909	−773.0366	−5.58	−5.71	3.10	3.03
AC…(H_2O)c	−770.9924	−773.0376	−6.34	−6.34	3.82	3.45
AC…(H_2O)d	−770.9919	−773.0366	−6.09	−5.52	1.04	0.86
AC…(H_2O)e	−770.9919	−773.0373	−6.02	−6.02	1.03	1.35
AC…(H_2O)$_7$	−1228.7202	−1231.8570	−43.86	−45.06	0.38	0.89

intermolecular interaction of triazole nitrogen N9 with water of theophylline has resulted in the hydrogen bond distance of 1.68 Å whereas in the present study, the same interaction is observed to be 2.00 Å. Hence, the replacement of C-H by nitrogen in theophylline has resulted in the enhancement of bond length.

In monohydrated AC, three closed complexes AC…H_2O (c), AC…H_2O(e) and AC…H_2O(f), and two open complexes AC…H_2O(a) and AC…H_2O(b) are formed (Figure S9). The molecular geometry of AC is not very sensitive to interactions with water due to the presence of weak donors and hence a lesser interaction energy. The highest interaction energy of 6.34 kcal mol^{-1} has been observed for AC…H_2O(c) at MP2 and B3LYP level of theory and much larger variation has not been observed in the interaction energy values for the other complexes (Table 6). The interaction energy order is AC…H_2O(c) > AC…H_2O(d) > AC …H_2O(e) > AC …H_2O(b) > AC…H_2O(a) at MP2 and AC …H_2O(c) > AC …H_2O(e) > AC …H_2O(b) > AC …H_2O(d) > AC …H_2O(a) at B3LYP level of theory. A prior study on monohydrated caffeine [49] has resulted in the interaction energy of 5.74, 5.06 and 6.21 kcal mol^{-1} for the interaction of water with imidazole nitrogen N9, carbonyl oxygen O11 and O13 of urea and amide moiety at an intermolecular distance of 1.96, 1.95 and 1.91 Å. The interaction of carbonyl oxygen O13 of amide moiety with water has resulted in the highest interaction energy value in caffeine whereas, the interaction of triazole nitrogen N9 with water is said to possess the highest value in 8-azacaffeine.

Overall, the formation of strong N-H…O bond has resulted in the highest interaction energy among the monohydrates and hence it is the preferred site for hydrogen bonding.

The calculated interaction energies of heptahydrated complexes summarized in Table 6 shows that the N7 protonated AX2… $(H_2O)_7$ tautomer has the highest interaction energy of 67.90 kcal mol^{-1} at MP2/6-311++G(d,p) and 71.66 kcal mol^{-1} at B3LYP/6-311++G(d,p) level of theory. This appears to be as a result of the variation in the strength of the hydrogen bonds existing in the tautomers. On going from 8-azaxanthine to 8-azatheophylline tautomers, the interaction energy of AT2… $(H_2O)_7$ is about 1-2 kcal mol^{-1} higher than AT1… $(H_2O)_7$ as observed for 8-azaxanthine. Further, 8-azacaffeine is said to possess the least interaction energy value of 43.86 and 45.06 kcal mol^{-1} at both levels of theory compared to 8-azaxanthine and 8-azatheophylline. Overall, the mono and heptahydrated caffeine complexes have the lowest interaction energy due to the presence of weak donors.

The energetic characteristics of the monohydrated complexes for the ground state calculated at MP2/6-311++G(d,p) and B3LYP/6-311++G(d,p) level of theory are displayed in Table 6. The energy profiles associated with the tautomerization processes of monohydrated complexes are given in Fig. 4. The stability of the tautomers is greatly affected by water. An analysis of the total energies of the monohydrates reveals that these values generally correlate well with the interaction energy between the modified nucleobase and water. In majority of the monohydrated complexes, it is to be noted that the interaction of water with the proton of triazole nitrogen decides the stability of the tautomers. Therefore, we can assume that the relative stability of the monohydrate depends on the tautomeric form of the triazole ring and almost does not depend on proton transfer within the substituted pyrimidine fragment. Inspection of the relative stability of the heptahydrated complexes given in Table 6 reveals that the N8 protonated AX1…$(H_2O)_7$ tautomer is better hydrated than AX2…$(H_2O)_7$ at both approaches. Similiar results have been obtained for 8-azatheophylline where, AT1…$(H_2O)_7$ is found to be more stable than AT2…$(H_2O)_7$ upon hydration. The order of stability of two protomeric forms of the hydrated complexes is AX1…$(H_2O)_7$ > AX2…$(H_2O)_7$ and AT1… $(H_2O)_7$ > AT2…$(H_2O)_7$ at MP2 and B3LYP level of theory, respectively.

Dipole moment

The ground state dipole moment values of the isolated forms of 8-azaxanthine, 8-azatheophylline and 8-azacaffeine in gas phase summarized in Table 2 shows that the most stable tautomers protonated at triazole nitrogen N8 in 8-azaxanthine and 8-azatheophylline possess the highest value of dipole moment than N7 protonated tautomers. Further, it is to be observed that the substitution of methyl group at pyrimidine N1 and N3 of 8-azaxanthine decreases the dipole moment values (8-azatheophylline). The effect is however not significant in 8-azacaffeine. Further, dipole moments are sensitive to the polarity of the medium. It is interesting to note the enhancement of dipole moment values in the solvent phase. The earlier studies also show that the dipole moment would be enhanced during the formation of hydrogen bonds [50]. Interaction of water molecule introduces significant changes in the dipole moment of the complexes (Table 6).

Frontier molecular orbitals of hydrated complexes

The nature of the HOMO and the LUMO for the most and the least stable monohydrated complexes corresponding to the ground state are shown in Fig. S10 (supplementary material) and for heptahydrated complexes in Fig. 5. It is evident that the nature of the HOMO is similar for both isolated and hydrated complexes. It must be noted that the orbital contamination from the water molecule is not found for the hydrated complexes. The examination of LUMOs for the hydrated complexes reveals that the N8 protonated tautomers have similar features which are different from those of the LUMOs of N7 protonated tautomers of 8-azaxanthine and 8-azatheophylline. The difference in the localization of the LUMO appears responsible for the distinct type of the structural deformation.

Hydrogen bond analysis

Each aza molecule links neighboring water molecules using the following four intermolecular hydrogen bonds N-H…O, O-H…N, O-H…O and C-H…O. These intermolecular hydrogen bonds can be detected and characterized using the AIM theory [51, 52]. The AIM calculation yielded the value of electron densities of monohydrated complexes to be 0.021 to 0.031 a.u. (N-H…O), 0.011 to 0.026 a.u. (O-H… N), 0.015 to 0.028 a.u. (O-H…O) and 0.007 to 0.012 a.u. (C-H…O), markedly lower than the other conventional bonds. For the heptahydrated complexes (Tables 7 and S4), the value of electron density for conventional N-H… O, O-H…N, O-H…O and C-H…N are from 0.026 to 0.064 a.u., 0.018 to 0.030 a.u., 0.016 to 0.038 a.u. and 0.006 to 0.015 a.u., respectively. These results suggest the existence of intermolecular hydrogen bonds in the two protomeric forms of 8-azaxanthine, 8-azatheophylline and in 8-azacaffeine as the topological criteria proposed by Koch and Popelier [53] are fulfilled. These values are within the range determined for hydrogen bonded complexes, which typically varies from 0.002 to 0.34 a.u [53, 54]. Among the monohydrated complexes, the structure with minimum bond length is said to possess the higher value of electron density and hence the higher stability in accordance with the relative energy values. It is to be observed that the electron density

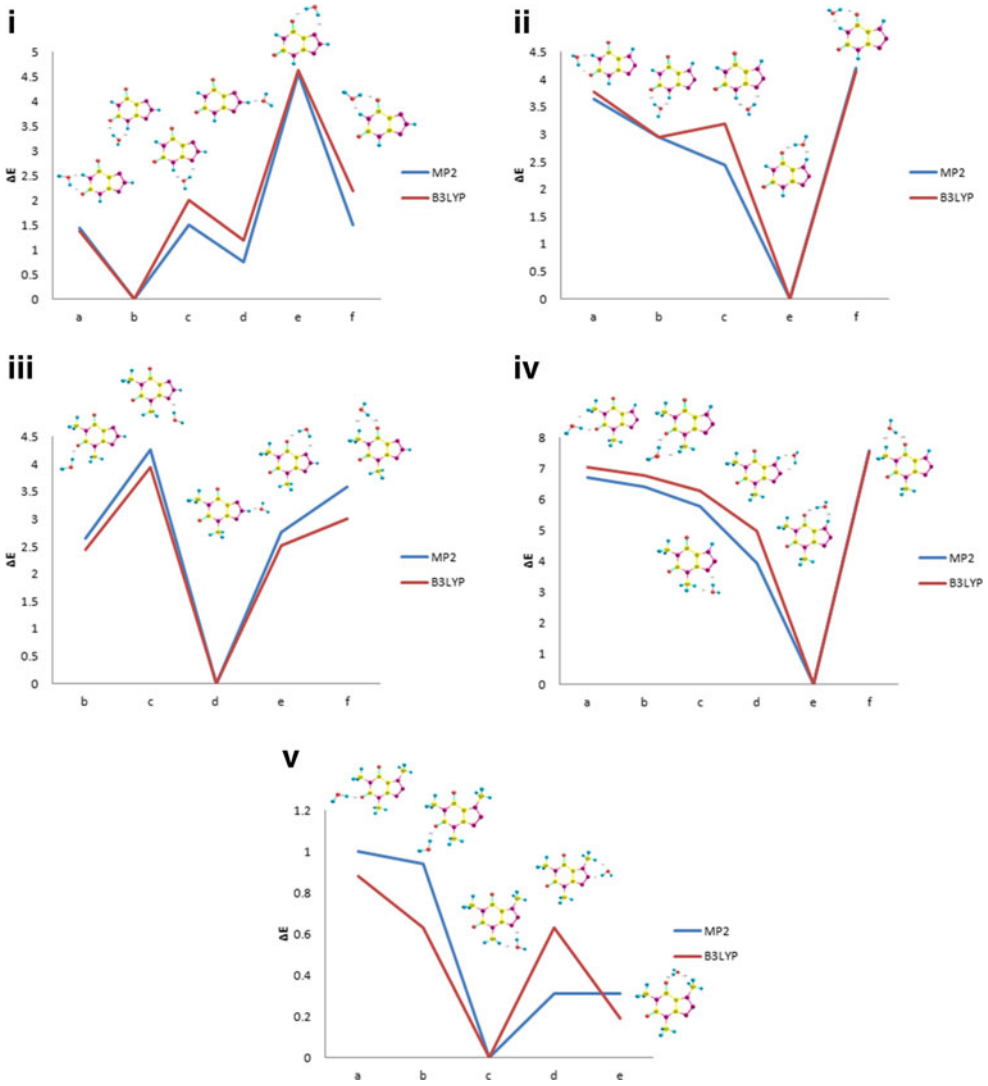

Fig. 4 Energy profile for the monohydrated complexes: (i) AX1 (ii) AX2 (iii) AT1 (iv) AT2 (v) AC Relative energies in kcal mol^{-1}

of conventional bonds is greater in heptahydrated complexes than monohydration resulting in stronger bonds. Overall, the electron density of N7 protonated tautomers is higher than N8 protonated tautomers among the two protomeric forms of 8-azaxanthine and 8-azatheophylline. On the basis of the calculated local potential energy density at BCPs, the following ordering of the intermolecular hydrogen bonds according to increasing bond strength can be proposed:

$$N-H\ldots O > O-H\ldots O > O-H\ldots N > C-H\ldots O.$$

In accordance with small electron densities, positive values of $\nabla^2\rho$ at BCPs indicate that the nature of hydrogen bonding in all the complexes is electrostatic. The hydrogen bond length and laplacian of electron density also reveal an inverse correlation. The curves corresponding to the correlation fit are shown in Figs. S11 and S12 with a correlation coefficient of 0.979 and 0.946 for electron density and 0.980 and 0.971 for laplacian of electron density with hydrogen bond length for mono and heptahydrated complexes.

Comparison of NBO results with the isolated molecules shows that the increase in occupancy of the σ*(N-H) orbital for monohydrated complexes lie in the range 0.010 to 0.024e, and that of σ*(O-H) from 0.003 to 0.020e for O-H…N, 0.006 to 0.022e for O-H…O and σ*(C-H) of 0.001 to 0.007e for C-H…O type hydrogen bonds. For heptahydration, there is a larger increase in occupancy of the antibonding orbitals of the conventional bonds where σ*(N-H) orbital lies from 0.020 to 0.083e, σ*(O-H) from 0.012 to 0.026e for O-H…N, 0.006 to 0.038e for O-H…O and σ*(C-H) of 0.001 to 0.007e for C-H…O type hydrogen bonds (Tables 7 and S4). This can be related to the elongation of the X-H bond. The charge is transferred between the interacting orbitals and hence the X-H antibond occupation values (X=N, O) of proton donor are found to be higher for all the bonds. It is revealed that the reduction in lone pair electron

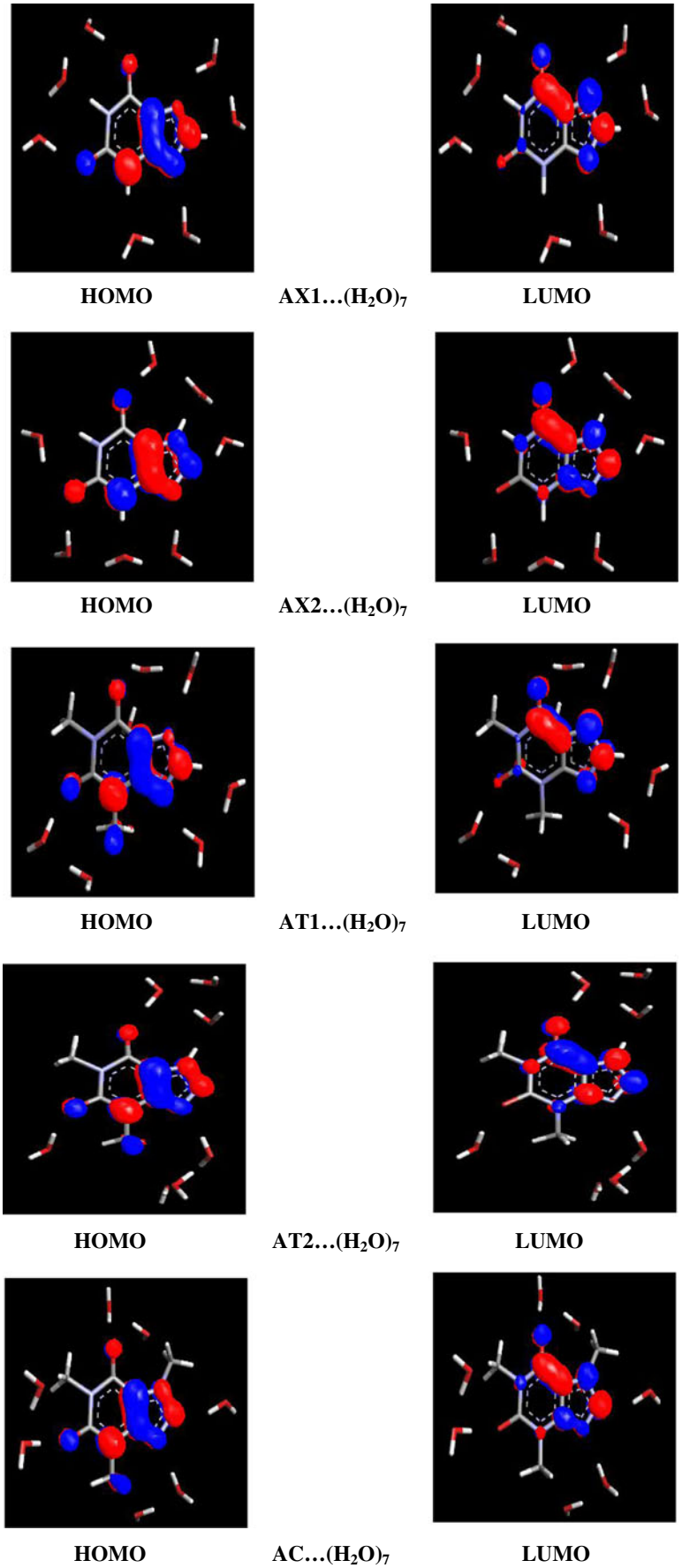

Fig. 5 Ground state HOMO and LUMO orbitals of heptahydrated AX1, AX2, AT1, AT2 and AC complexes

Table 7 Geometrical parameters (bond lengths in Å, bond angles in degrees), electron density ρ (a.u.), laplacian of electron density $\nabla^2\rho$ (a.u.), ellipticity ε, the occupation number of lone pair in the proton acceptor n(Y) and of antibonds of proton donor n[σ*(X-H)] and the corresponding stabilization energies $E^{(2)}$ (kcal mol^{-1}) involved in hydrogen bonds in heptahydrated AX2, AT2 and AC corresponding to the ground state calculated at B3LYP/6-311G++(d,p) level of theory. For labeling of atoms see Fig. S11

Complex	Hydrogen bond	$R_{X-H\ (X=N,O,C)}$		$R_{H\ldots Y}$	ΔR_{X-H}[a]	$R_{X\ldots Y}$	<X-H…Y	ρ(r)	$\nabla^2\rho(r)$	ε	n(Y)	n[σ*(X-H)]	$E^{(2)}$
		Monomer	Complex										
AX2…$(H_2O)_7$	N1-H12…O15	1.0130	1.0259	1.9289	0.0129	2.8434	146.8	0.026	0.096	0.037	1.976	0.032(0.012)	9.43
	N3-H10…O21	1.0100	1.0565	1.6342	0.0465	2.6892	176.1	0.055	0.137	0.059	1.919	0.088(0.014)	36.13
	N7-H14…O30	1.0110	1.0670	1.5806	0.0560	2.6440	174.0	0.064	0.141	0.052	1.905	0.100(0.017)	43.42
	O24-H25…N9	0.9653	0.9779	1.9725	0.0126	2.9215	163.0	0.027	0.084	0.053	1.922	0.024(0.000)	9.28
	O27-H28…N8	0.9653	0.9711	2.1422	0.0058	3.0110	148.2	0.018	0.061	0.059	1.947	0.012(0.000)	3.40
	O15-H17…O11	0.9653	0.9718	2.0005	0.0065	2.8024	138.4	0.023	0.083	0.029	1.858	0.014(0.000)	3.81
	O18-H19…O11	0.9653	0.9749	1.9091	0.0096	2.8700	168.1	0.026	0.095	0.020	1.858	0.019(0.000)	5.11
	O21-H22…O18	0.9653	0.9723	1.9360	0.0070	2.7671	142.0	0.025	0.096	0.069	1.982	0.015(0.000)	6.40
	O21-H23…O24	0.9653	0.9751	1.8890	0.0098	2.7787	150.4	0.028	0.102	0.034	1.976	0.022(0.000)	9.37
	O30-H32…O27	0.9653	0.9707	2.0229	0.0054	2.8243	138.5	0.021	0.079	0.036	1.987	0.011(0.000)	4.43
	O30-H31…O33	0.9653	0.9780	1.8366	0.0127	2.7418	152.6	0.031	0.113	0.041	1.972	0.026(0.000)	11.43
	O33-H35…O13	0.9653	0.9756	1.8767	0.0103	2.8446	171.1	0.027	0.102	0.042	1.865	0.019(0.000)	4.74
AT2…$(H_2O)_7$	N7-H14…O24	1.0100	1.0513	1.6657	0.0413	2.7166	178.2	0.050	0.134	0.043	1.929	0.078(0.017)[b]	31.98
	O27-H29…N9	0.9653	0.9747	1.9899	0.0094	2.9560	170.7	0.026	0.082	0.038	1.924	0.021(0.000)	8.21
	O36-H38…O11	0.9653	0.9694	1.9242	0.0041	2.8717	165.1	0.023	0.095	0.055	1.972	0.013(0.000)	3.26
	O21-H23…O13	0.9653	0.9792	1.7816	0.0139	2.7581	174.8	0.032	0.126	0.019	1.965	0.025(0.000)	7.50
	O24-H26…O21	0.9653	0.9704	2.0498	0.0051	2.8699	141.0	0.021	0.074	0.037	1.987	0.011(0.000)	4.09
	O39-H41…O21	0.9653	0.9727	1.9407	0.0074	2.8266	150.2	0.024	0.093	0.065	1.982	0.015(0.000)	6.18
	O30-H32…O27	0.9653	0.9856	1.7821	0.0203	2.7188	157.5	0.038	0.119	0.020	1.956	0.038(0.000)	16.25
	O33-H35…O30	0.9653	0.9752	1.9223	0.0099	2.7923	147.2	0.026	0.095	0.052	1.978	0.019(0.000)	7.64
	O27-H28…O33	0.9653	0.9697	2.0677	0.0044	2.8671	138.5	0.019	0.072	0.009	1.989	0.008(0.000)	3.25
	O24-H25…O39	0.9653	0.9738	1.9699	0.0085	2.8022	142.0	0.024	0.088	0.069	1.984	0.013(0.000)	5.55
	C10-H16…O30	1.0902	1.0913	2.6710	0.0011	3.5366	135.8	0.006	0.019	0.052	1.995	0.011(0.010)	0.50
	C10-H15…O33	1.0902	1.0876	2.7327	-0.0026	3.4805	125.6	0.006	0.019	0.083	1.995	0.007(0.010)	0.33
AC…$(H_2O)_7$	O24-H25…N8	0.9653	0.9693	2.0678	0.0040	2.9705	154.2	0.022	0.074	0.050	1.944	0.014(0.000)	5.03
	O27-H28…N9	0.9653	0.9780	1.9244	0.0127	2.8975	172.9	0.030	0.091	0.036	1.917	0.026(0.000)	10.76
	O33-H35…O11	0.9653	0.9734	1.8664	0.0081	2.8309	170.5	0.026	0.107	0.023	1.969	0.016(0.000)	4.98
	O39-H41…O13	0.9653	0.9728	1.8676	0.0075	2.8248	167.3	0.026	0.106	0.080	1.970	0.016(0.000)	4.76
	O30-H31…O27	0.9653	0.9760	1.8427	0.0107	2.7950	164.4	0.031	0.111	0.035	1.973	0.024(0.000)	11.13
	O36-H38…O33	0.9653	0.9756	1.8549	0.0103	2.8021	162.9	0.029	0.108	0.057	1.974	0.023(0.000)	10.56
	O42-H43…O39	0.9653	0.9763	1.8416	0.0110	2.7986	165.9	0.031	0.111	0.036	1.972	0.024(0.000)	11.45
	C14-H23…O42	1.0890	1.0917	2.1849	0.0027	3.2652	169.7	0.015	0.055	0.095	1.989	0.015(0.009)	3.89
	C10-H17…O30	1.0874	1.0905	2.2934	0.0031	3.2953	151.9	0.013	0.043	0.076	1.991	0.013(0.006)	2.47
	C12-H19…O36	1.0899	1.0919	2.2997	0.0020	3.3743	167.6	0.013	0.041	0.055	1.990	0.015(0.009)	2.98

[a] $\Delta R_{X-H} = R_{X-H}$ (Complex) - R_{X-H} (Monomer)

[b] The numbers in parenthesis indicate corresponding values of monomers calculated using same basis set as in complex

density is indeed accompanied by a small increase in electron density in the σ^* antibonding orbital. Specifically, the maximum elongation in bond length observed for N-H of N-H…O bond is linearly correlated to the increase in occupation of the σ^*(N-H) orbitals.

For each donor and acceptor, the stabilization energy $E^{(2)}$ associated with hydrogen bonding between sites i and j is given by the following equation,

$$E^{(2)} = q_i \frac{F^2(i,j)}{\varepsilon_i - \varepsilon_j}$$

where q_i is the *i*th donor orbital occupancy, ε_j, ε_i are the diagonal elements (orbital energies) and *F(i,j)* are off diagonal elements associated with NBO Fock matrix. The $E^{(2)}$ term corresponding to hydrogen bond interactions can be considered as the total charge transfer energy. If the stabilization energy between a donor bonding orbital and an acceptor bonding orbital is large, there is a strong interaction between the two bonds. Among the monohydrated complexes, the strongest interaction existing between n(O15) and σ*(N8-H14) of AX1…H_2O(d), n(O15) and σ*(N7-H14) orbital of AX2…H_2O(f) correspond to stabilization energy of 14.36 and 11.77 kcal mol^{-1}, respectively. Further, in AT1 and AT2, n(O21) →σ^*(N8-H14) of AT1…H_2O(d,e) and n(O21) →σ^*(N7-H14) of AT2…H_2O(f) interactions play an important role in stabilization of the complex resulting in the stabilization energy of 13.70 and 12.48 kcal mol^{-1}, respectively. Similarly, the lone pairs of the acceptor atoms N8 in AC…H_2O(c) offer their electron to σ*(O24-H25) antibond of 8-azacaffeine and thus they have a stabilization energy of 8.07 kcal mol^{-1}. Hence it is to be observed that N-H…O bonds surpass all other interactions in accordance with the charge transfer effect. The stabilization energy presented in Tables 7 and S4 for heptahydrated complexes reveal a maximum stabilization energy of 43.42 kcal mol^{-1} for AX2…$(H_2O)_7$. The lone pairs of the acceptor atoms O30 in AX2…$(H_2O)_7$ offer their electrons to the σ*(N7-H14) and thus they have the highest value of stabilization energy. Similarly N7 protonated tautomer AT2…$(H_2O)_7$ possesses the highest stabilization energy value of 31.98 kcal mol^{-1} due to the existence of strong interaction between n(O24) and σ*(N7-H14). However, heptahydrated 8-azacaffeine AC…$(H_2O)_7$ possesses the lowest value of stabilization energy compared to other complexes.

Conclusions

The TD-DFT and CIS calculations are performed to investigate the electronic structure and spectral properties of 8-azaxanthine, 8-azatheophylline and 8-azacaffeine in gas and solvent phases. Substitution has significant effect on the properties of 8-azaxanthine. Among the two protomeric forms of 8-azaxanthine and 8-azatheophylline, the N8 protonated tautomers are found to be more stable than the N7 protonated tautomers which are in agreement with the earlier studies on the solid state. The substitutions alter the spatial charge distribution of the frontier molecular orbitals, and hence the spectral properties depend upon the substitution. The TD-DFT results show that for all the isolated complexes, the lowest energy transition is due to the excitation from HOMO to LUMO. The emission spectra calculated using TD-B3LYP method in solvent phase is in accordance with the experimental values and the spectra are red shifted relative to absorption. It is interesting to note that the absorption and emission energy corresponding to H→L transition is comparable with the energy gap value. The molecules with a small H→L energy gap possess maximum absorption and emission wavelength.

Hydration has significant influence on the geometry and stability of aza complexes. The mono and heptahydrated 8-azaxanthine and 8-azatheophylline complexes protonated at N7 results in higher interaction energy than N8 protonated tautomers. The relative stability of the monohydrates depends on the tautomeric form of the triazole ring and almost does not depend on the proton transfer within the substituted pyrimidine fragment. Dipole moments are sensitive to the polarity of the medium and an enhancement has been noted in the solvent phase. The electron density and its Laplacian at BCPs correlate well with the hydrogen bond length and augment the stability order. The maximum elongation in bond length observed for N-H…O bond is linearly correlated to the increase in occupation of the σ^*(N-H) orbitals resulting in the highest value of stabilization energy.

References

1. Maldonado CR, Quiros M, Salas JM (2009) First and second coordination spheres in divalent metal compounds containing pyridine and 4,6-dimethyl-1,2,3-triazolo[4,5-d]pyrimidin-5,7-dione. Polyhedron 28:911–916
2. Maldonado CR, Quiros M, Salas JM, Rodriguez-Dieguez A (2009) A study of the second coordination sphere in 8-azaxanthinato salts of divalent metal aquacomplexes. Inorg Chim Acta 362:1553–1558
3. Ravichandran V, Ruban GA, Chacko KK, Molina MAR, Rodriguez EC, Salas-Peregrin JM, Aoki K, Yamazaki H (1986) Crystal structures of an antiallergic 8-azapurine (*v*-triazolo[4,5-*d*] pyrimidine) and its metal complex, 3-methyl-8-azaxanthine monohydrate and trans-diamminebis (3-methyl-8-azaxanthinato)copper (II) dehydrate. J Chem Soc Chem Commun doi:10.1039/C39860001780
4. Purnell LG, Estes ED, Hodgson DJ (1976) Interaction of metal ions with 8-azapurines.II Synthesis and structure of bis(8-azahypoxanthinato)tetraaquocadmium (II). J Am Chem Soc 98:740–743
5. Graves BJ, Hodgson DJ (1981) Metal ion interactions with 8-azapurines-synthesis and structure of dichlorobis (8-azaadenine) mercury(II) and tetraaquabis (8-azahypoxanthinato) mercury(II). Inorg Chem 20:2223–2229

6. Gu J, Wang J, Leszczynski J (2004) H-bonding patterns in the platinated guanine-cytosine base pair and guanine-cytosine-guanine-cytosine base tetrad: an electron density deformation analysis and aim study. J Am Chem Soc 126:12651–12660
7. Vince R, Hua M (1990) Synthesis and anti-HIV activity of carbocyclic 2′,3′-didehydro-2′,3′- dideoxy 2,6-disubstituted purine nucleosides. J Med Chem 33:17–21
8. Albert A (1986) Chemistry of 8-Azapurines (1, 2, 3-Triazolo[4, 5-*d*] pyrimidines). Adv Heterocycl Chem 39:117–180
9. Brule G, Eckhardt SJ, Hall TC, Winkler A (1973) Drug therapy of cancer. World Health Organisation, Geneva
10. Schabel FM Jr (1968) The antiviral activity of 9-b-D-arabinofuranosyladenine (ara-A). Chemotherapy 13:321–338
11. Ward DC, Reich E (1969) Relationship between nucleoside conformation and bio-logical activity. Annu Rep Med Chem 5: 272–284
12. Grunberger D, Grunberger G (1979) In: Hahn FE (ed) Antibiotics, vol 2. Springer-Verlag, Berlin, pp 110–123
13. Shewach DS, Krawczyk SH, Acevedo OL, Townsend LB (1992) Inhibition of adenosine deaminase by azapurine ribonucleosides. Biochem Pharmacol 44:1697–1700
14. Franchetti P, Messini L, Cappellacci L, Grifantini M, Lucacchini A, Martini C, Senatore G (1994) 8-azaxanthine derivatives as antagonists of adenosine receptors. J Med Chem 37:2970–2975
15. Shoemaker AL, Hodgson DJ (1977) Structure of 7-methyl-8-azaadenine - crystallographic and molecular-orbital study. J Am Chem Soc 99:4119–4123
16. Singh P, Hodgson DJ (1977) 2-Azaadenosine hemihydrates. J Am Chem Soc 99:4807–4815
17. Lemay HE Jr, Hodgson DJ (1978) Antiallergenic 8-azapurines. Structural characterization of 9-diethylcarbamoyl-2-(2-propoxyphenyl)-8-azahypoxanthine. J Am Chem Soc 100:6474–6478
18. Wilson SR, Wilson RB, Shoemaker AL, Wooldridge KRH, Hodgson DJ (1982) Antiallergic 8-azapurines 3.Structural characterization of 2-(2-Proproxyphenyl)- 8- azahypoxanthine, 2-(2-propoxy-5-(propylsulfonyl) phenyl)-8-azahypoxanthine and 2-(2-propoxy-5-(N-methyl-N-isopropylsalfomoyl) phenyl-8-azahypoxanthine. J Am Chem Soc 104:259–264
19. Nubel G, Pfleiderer WP (1965) Purine V: Über die Synthese und Struktur von 8-Aza-xanthin (5.7-Dioxo-tetrahydro-ν-triazolo[4.5-d]pyrimidin) und seinen N-Methyl-Derivaten. Chem Ber 98: 1060–1072
20. L'abbe G, Persoons MA, Toppet S (1985) Study of the prototropic tautomerism of 8- azatheophylline by ^{13}C and ^{15}N NMR spectroscopy. Magn Res Chem 25:362–364
21. Sanchez MP, Romnero MA, Salas JM, Cardenas DJ, Molina J, Quiros M (1995) Molecular- orbital study of 8-azaxanthine derivatives and crystal-structure of 1,3-dimethyl-8-azaxanthine monohydrate. J Mol Struct 344:257–264
22. Wierzchowski J, Wielgus-Kutrowska B, Shugar D (1996) Fluorescence emission properties of 8-azapurines and their nucleosides, and application to the kinetics of the reverse synthetic reaction of purine nucleoside phosphorylase. Biochim Biophys Acta 1290:9–17
23. Wierzchowski J, Bzowska A, Stepniak K, Shugar D (2004) Interactions of calf spleen purine nucleoside phosphorylase with 8-azaguanine, and a bisubstrate analogue inhibitor: implications for the reaction mechanism. Z Naturforsch 59:713–725
24. Ito S, Takeshi T, Mori H, Teruo A (1981) A sensitive new method for measurement of guanase with 8-azaguanine in bicine bis-hydroxy ethyl glycine buffer as substrate. Clin Chim Acta 115:135–144
25. Perez-Vicente R, Alamillo JM, Cardenas J, Pineda M (1992) Purification and substrate inactivation of xanthine dehydrogenase from clamydomonus reinhardtii. Biochim Biophys Acta 1117:159–166
26. Colloc'h N, El Hajji M, Bachet B, L'Hermite G, Schiltz M, Prange T, Castro B, Mornon JP (1997) Crystal structure of the protein drug urate oxidase-inhibitor complex at 2.05 Å resolution. Nat Struct Biol 4:947–952
27. Retailleau P, Colloc'h N, Vivares D, Bonnete F, Castro B, El Hajji M, Mornon JP, Prange T (2004) Complexed and ligand-free high resolution structures of urate oxidase (Uox) from aspergillus flavus: a re-assignation of the active site binding mode. Acta Cryst D60:453–462
28. Medza G, Wierzchowski J, Kierdaszuk B, Shugar D (2009) Fluorescence emission properties of 8-aza analogues of caffeine, theophylline and N-alkyl xanthines. Bioorg Med Chem 17:2585–2591
29. Klymchenko AS, Demchenko AP (2003) Multiparametric probing of intermolecular interactions with fluorescent dye exhibiting excited state intramolecular proton transfer. Phys Chem Chem Phys 5:461–468
30. Maity SS, Samanta S, Sardar PS, Pal A, Dasgupta S, Ghosh S (2008) Fluorescence, anisotropy and docking studies of proteins through excited state intramolecular proton transfer probe molecules. Chem Phys 354:162–173
31. Casida ME (1995) In: Chong DP (ed) Recent advances in density functional methods, part I. World Scientific, Singapore
32. Gross EKU, Dobson JF, Petersilka M (1996) In: Nalewajski RF (ed) Density functional theory II. Springer, Heidelberg
33. Foresman JB, Head-Gordon M, Pople JA, Frisch MJ (1992) Toward a systematic molecular orbital theory for excited states. J Phys Chem 96:135–149
34. Wang D, Hao C, Wang S, Dong H, Qiu J (2012) Time-dependent density functional theory study on the electronic excited-state hydrogen bonding of the chromophore coumarin 153 in a room-temperature ionic liquid. J Mol Mod 18:937–945
35. Bader RFW (1990) Atoms in molecules, a quantum theory. Oxford University Press, Oxford
36. Gledening ED, Reed AE, Carpenter JA, Weinhold F, NBO Version 3.1
37. Becke AD (1998) Density-functional exchange-energy approximation with correct asymptotic Behavior. Phys Rev A 38:3098–3100
38. Lee C, Yang W, Parr RG (1988) Development of the Colle-Salvetti correlation-energy formula into a functional of the electron density. Phys Rev B 37:785–789
39. Moller C, Plesset MS (1934) Note on an approximation treatment for many-electron systems. Phys Rev 46:618–622
40. Miertus S, Scrocco E, Tomasi J (1981) Electrostatic Interaction of a solute with a continuum. A direct utilization of ab initio molecular potentials for the prevision of solvent effects. J Chem Phys 55:117–129
41. Boys SF, Bernardi F (1970) Calculation of small molecular interactions by differences of separate total energies - some procedures with reduced errors. Mol Phys 19:553–566
42. MORPHY98 (1998) A program written by Popelier PLA with a contribution from Bone UMIST RGA. Manchester, UK
43. Frisch MJ, Trucks GW, Schlegel HB, Scuseria GE, Robb MA, Cheeseman JR et al. (2003) Gaussian03, Revision B.05. Gaussian, Inc, Pittsburgh
44. Madariaga ST, Contreras JG (2003) Interaction energies in non Watson-Crick pairs: an *ab initio* study of g·u and u·u pairs. J Chil Chem Soc 48:129–133
45. Smith EDL, Hammond RB, Jones MJ, Roberts KJ, Mitchell JBO, Price SL, Harris RK, Apperley DC, Cherryman JC, Docherty R (2001) The determination of the crystal structure of anhydrous theophylline by X-ray powder diffraction with a systematic search algorithm, lattice energy calculations, and C-13 and N-15 solid-state NMR: a question of polymorphism in a given unit cell. J Phys Chem B 105:5818–5826
46. Wierzchowski J, Sepiol J, Sulikowski D, Kierdaszuk B, Shugar D (2006) Fluorescence emission properties of 8-azaxanthine and its N-

alkyl derivatives: excited-state proton transfer, and potential applications in enzymology. J Photochem Photobiol A–Chem 179:276–282
47. Valeur B (2002) Molecular fluorescence, principles and applications. Wiley-VCH, Weinheim
48. Kryachko ES (2006) In: Grabowski SJ (ed) Hydrogen bonding-new insights. Springer, Dordrecht
49. Balbuena PB, Blocker W, Dudek RM, Cabrales-Navarro FA, Hirunsit P (2008) Vibrational spectra of anhydrous and monohydrated caffeine and theophylline molecules and Crystals. J Phys Chem A 112:10210–10219
50. Karthika M, Senthilkumar L, Kanakaraju R (2012) Theoretical investigations on 6,8-dithioguanine tautomers. Struct Chem 23:1203–1218
51. Karthika M, Senthilkumar L, Kanakaraju R (2012) Theoretical studies on hydrogen bonding in caffeine-theophylline complexes. Comput Theoret Chem 979:54–63
52. Senthilkumar L, Ghanty TK, Ghosh SK (2005) Electron density and energy decomposition analysis in hydrogen-bonded complexes of azabenzenes with water, acetamide, and thioacetamide. J Phys Chem A 109:7575–7582
53. Koch U, Popelier PLA (1995) Characterization of C-H-O Hydrogen Bonds based on the Charge Density. J Phys Chem 99:9747–9754
54. Popelier PLA, Bader RFW (1992) The existence of an intramolecular C-H-O hydrogen bond in creatine and carbamoyl sarcosine. Chem Phys Lett 189:542–548